Morphological and optical properties of MgO$_{1-x}$ZnS$_x$ thin films

H. S. Al-Rikabi[a], M. H. Al-Timimi[a,*], W. H. Albanda[b]
aPhysics Department ,College of Science, Diyala University, Diyala, Iraq
bScience Department - College of Basic Education - Al-Mustansiriya University, Iraq

(MgO) films doped with (ZnS) were prepared using a spray pyrolysis technique. Thin films were deposited on glass substrates at (350°C) with different concentrations (0,2,4,6,8) % of ZnS to study the surface morphology and optical properties. The (AFM) images indicated that increasing the (ZnS) concentrations leads to a decrease in the surface roughness rate. The optical measurements showed a decrease in the transmittance and reflectivity spectrum of all the prepared films, with an increase in (ZnS) concentrations and an increase in the absorption coefficient, refractive index, and extinction coefficient. The values of the real part of the dielectric constant were higher compared to the imaginary part for all the prepared films. Also, the optical energy gap decreased with the increase of (ZnS) concentrations within the range of (2.771-2.549) eV.

1. Introduction

Thin (MgO) films attract great scientific and technological interest due to their important application properties [1]. An important application of (MgO) films is used in sensors, electronic devices, solar cells, and LEDs [1-3]. Magnesium oxide has thermal and chemical stability and a wide bandgap [1, 2]. In general, dopants are useful for significantly modifying the properties of host materials. Several dopings have been used to modify the properties of MgO thin films, such as (Zn, Ag, Al, Fe, and Cr) [4-8]. We chose ZnS as the doping component in this work because (ZnS) is a low-toxicity, readily available, and low-cost material [9]. Moreover, (ZnS) is a composite (II-VI) semiconductor with a bandgap (3.72 eV at room temperature) and a high refractive index that is used in many different technological applications [10]. (MgO) thin films can be deposited by several techniques, including (sol-gel) [11], (CVD) chemical vapor deposition [12], electron-beam evaporation [4, 13], spraying [5], spin coating [14], spray pyrolysis technique [15], etc. Compared to these methods, the spray pyrolysis technique is simple in cost and can deposit large-area films [16, 17]. Therefore, the present work investigates how to modify the morphology and optical properties of (MgO) thin films deposited by spray pyrolysis technique and doped with (ZnS).

2. Experimental part

(MgO) thin films saturated with (ZnS) sulfide were prepared by the spray pyrolysis method. Magnesium chloride (MgCl$_2$.6H$_2$O), zinc nitrate (Zn(NO$_3$).6H$_2$O), and thiourea (CH$_4$N$_2$S) dissolved in 0.1M distilled water was used. (MgO) was doped with different volumetric ratios (0,2,4,6,8) % of (ZnS). The solution was sprayed onto glass substrates at (350 °C) using a compressor at (1.5 bar). The surface morphology of the thin films was detected by atomic force microscopy (AFM). The optical properties were measured using an ultraviolet-visible (UV-Vis) spectrophotometer.

3. Results and discussion

3.1. Surface morphological

Fig. 1 Shows the images of the results of the (AFM) tests for all the prepared films. The topography of the thin films ($MgO_{1-x}ZnS_x$) was studied with different doping ratios using atomic force microscopy (AFM). The (AFM) images indicated that the surface morphology strongly depends on the doping concentration in the prepared thin films. The decrease in surface roughness is due to the reduction of the average crystallite size of (MgO) films after (ZnS) replacement [18-20]. Also, the more extensive grain formation may lead to a decrease in surface roughness [21]. Fig. 2 Shows the rate of surface roughness and particle size as a function of the doping percentage with (ZnS). The smallest value of (Sa) for the film doped with (6%) of (ZnS). Table 1. shows the surface roughness and particle size values with an increasing percentage of doping with (ZnS).
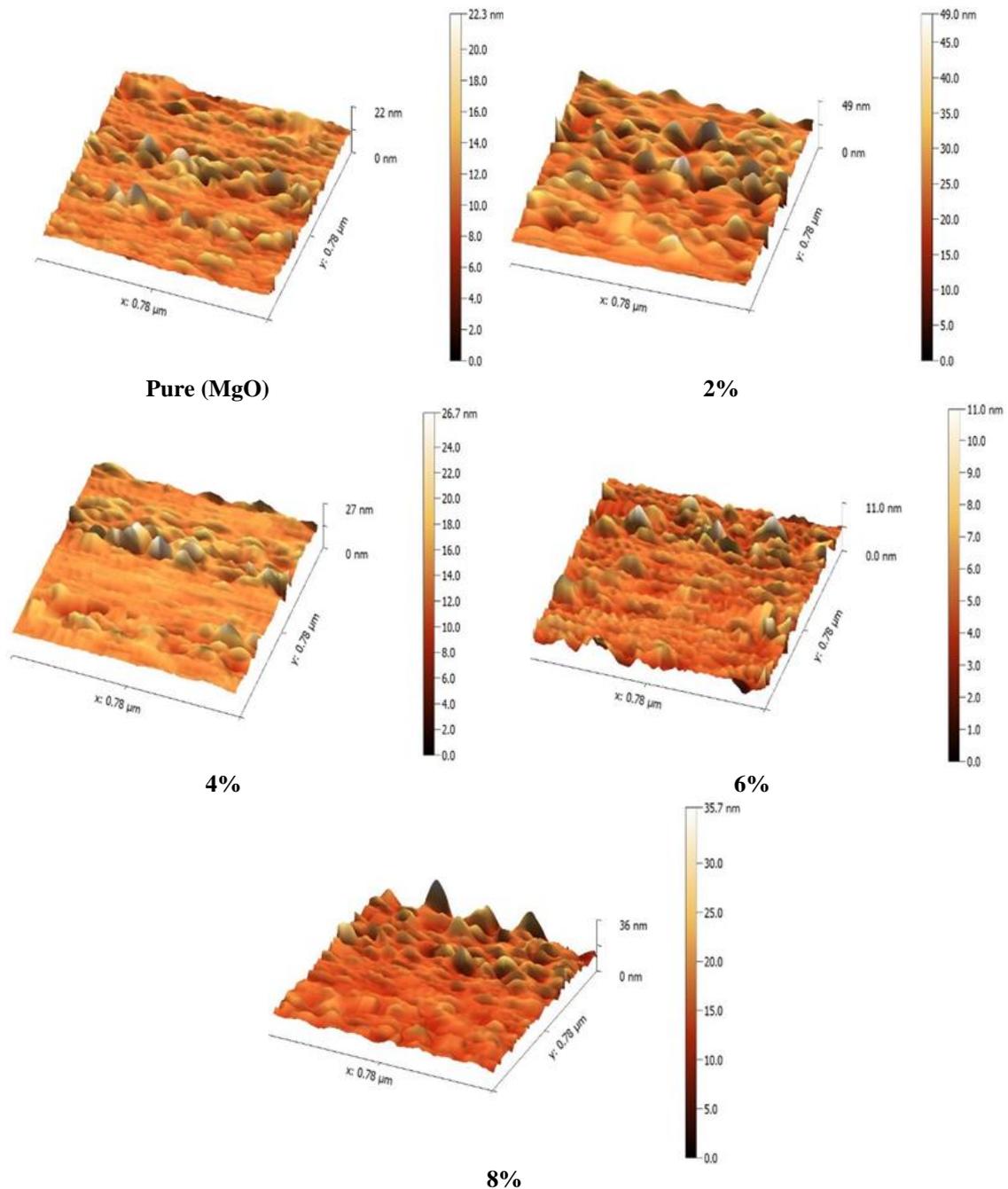
Pure (MgO)   **2%**

4%   **6%**

8%

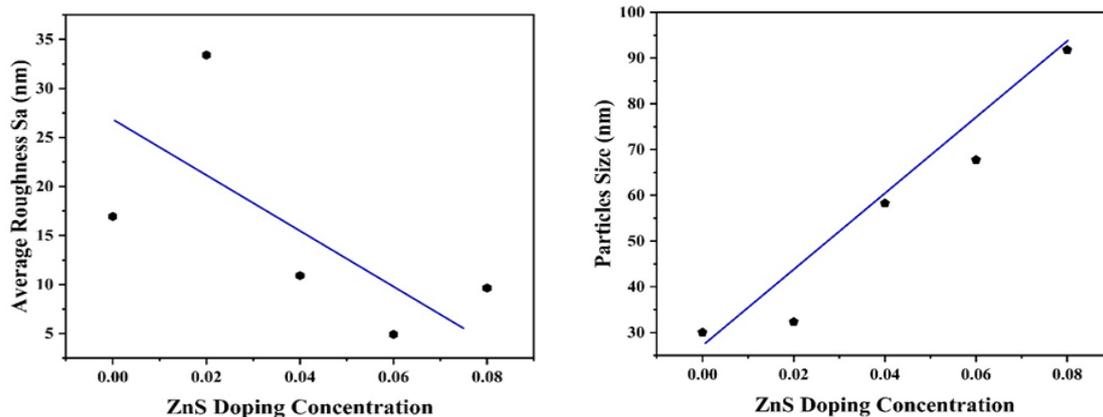*Fig. 1. AFM images of MgO_{1-x}ZnS_x films.*

Fig. 2. Average roughness and particle size of MgO$_{1-x}$ZnS$_x$ films.

Table 1. Roughness and (RMS) for (MgO$_{1-x}$ZnS$_x$) films.

Samples	Roughness Average Sa (nm)	RMS (nm)	Particles Size (nm)	Surface Skewness (Ssk) (nm)	Surface Kurtosis (Sku) (nm)	Maximum Height Sz(nm)
MgO	16.94	25.02	30.05	-0.8114	5.018	16.31
MgO$_{0.98}$ZnS$_{0.02}$	33.41	42.71	32.35	-1.111	3.596	20.27
MgO$_{0.96}$ZnS$_{0.04}$	10.91	12.69	58.27	-0.5094	2.237	69.61
MgO$_{0.94}$ZnS$_{0.06}$	4.922	6.037	67.77	-0.4426	3.314	35.15
MgO$_{0.92}$ZnS$_{0.08}$	9.641	12.59	91.80	-0.00182	3.245	80.98

3.2. Optical properties

Fig. 3 Shows the transmittance spectrum of the prepared thin films. The transmittance values decreased with the increase in the doping percentage with (ZnS). This is in agreement with researchers Harun GÜNEY and Fuad T. Ibrahim [22, 23]. This decrease in transmittance is attributed to the increased absorption caused by the rise in (ZnS) concentration in the thin film. Improving the content of (ZnS) leads to an increase in the density of the localized states and, thus, the sample becomes more opaque to the incident light. This leads to a shift of the absorption edge towards lower energies (high wavelengths). In this region, the photons have enough energy to excite electrons from the valence band to the conduction band. Thus, photons are absorbed into the thin film material [23, 24]. Also, the formation of new energy levels near the conduction band leads to an increase in the number of electrons that reach the conduction band, thus reducing the energy gap with an increase in absorbance and a decrease in transmittance values [8, 25].
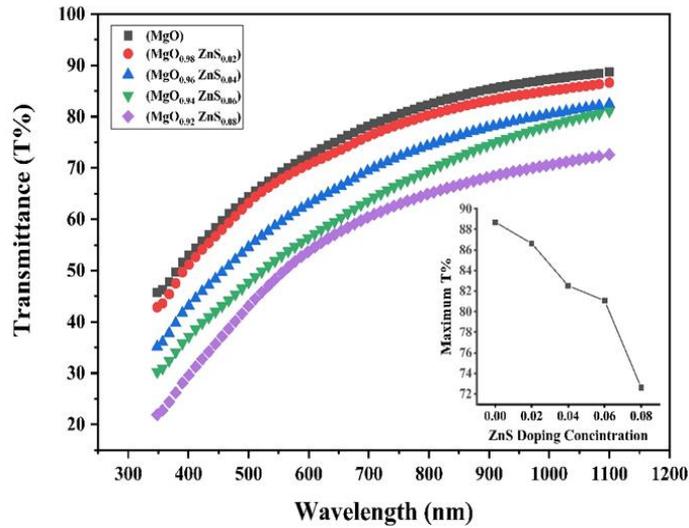
Fig. 3. Transmittance spectra of (MgO$_{1-x}$ZnS$_x$) thin films. Inset figure shows the maximum transmittance with (ZnS) doping Concentration.

Fig. 4 shows the reflectivity values (R), as the reflectivity values decreased with the increase in the percentage of doping with (ZnS). The absorption coefficient (α) was calculated from the relationship (1) [24, 26, 27]. Fig. 5 Shows the absorption coefficient, and We note that the values of the absorption coefficient (α > 10^4 cm^{-1}) confirm the occurrence of the allowed direct electronic transitions [28].

$$\alpha = 2.303A/t \tag{1}$$

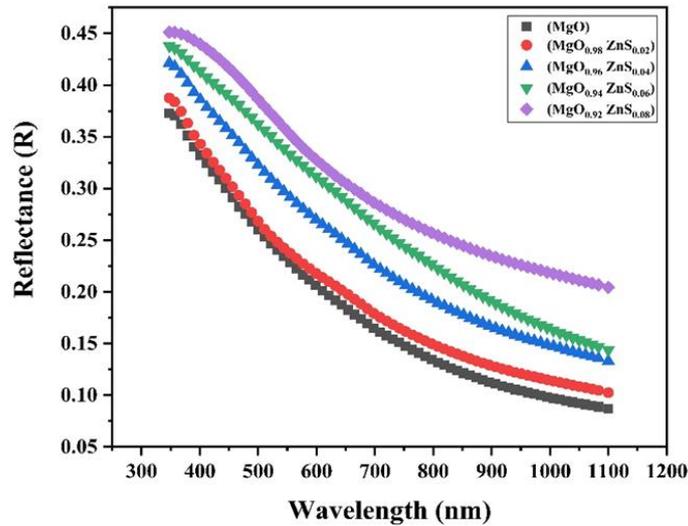(A) and (t) represents the film's absorbance and thickness.

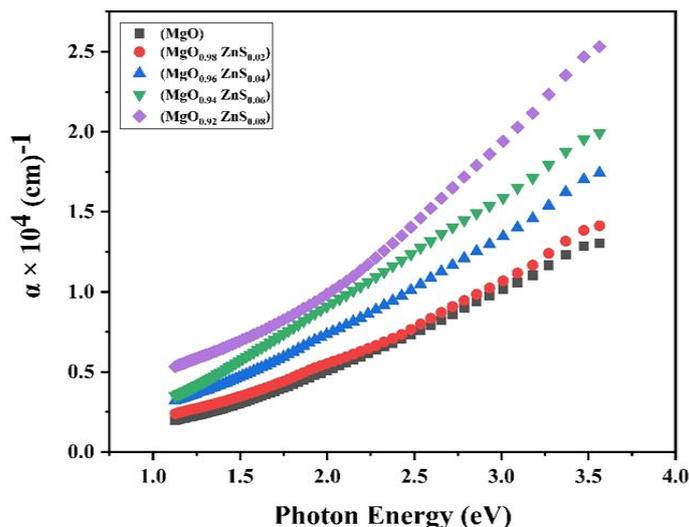*Fig. 4. Reflectance of (MgO$_{1-x}$ZnS$_x$) thin films.*

Fig. 5. Absorption Coefficient of (MgO$_{1-x}$ZnS$_x$) thin films.

The optical energy gap of the allowed direct electronic transitions was calculated from the relation (2) [29, 30]. Fig. 6 Shows the relationship between (αhυ)^2 and the incident photon's energy. The optical energy gap of the films decreases with the increase in the percentage of doping with (ZnS), and it is within the range of (2.549-2.771) eV, Our results are in agreement with the findings of researchers Sabiha Aksay and Ahmet Taşer [31, 32]. The decrease in the energy gap is the formation of local energy levels close to the conduction band, contributing to the increase in the number of electrons in the conduction band [33].

$$(\alpha h\upsilon) = A(h\upsilon - E_g)^r \tag{2}$$

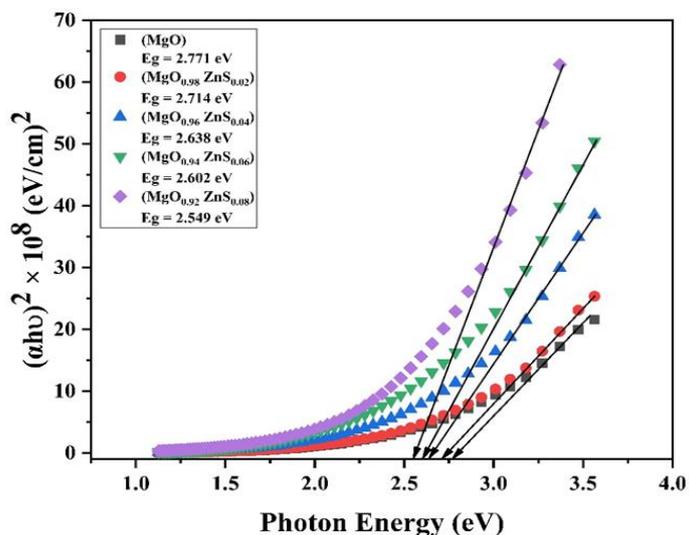(Eg) Energy gap, (A) constant, and (r) equal to (1/2) for allowed direct transitions.

Fig. 6. Energy Gap of (MgO$_{1-x}$ZnS$_x$) thin films.

The extinction coefficient (k$_o$) was calculated from the relationship (3) [34, 35]. Fig. 7 Shows the extinction coefficient, The extinction coefficient increases with the increase in the percentage of ZnS doping. and the refractive index (n$_o$) was also calculated from the relationship (4) [36], Shown in Fig. 8. We note an increase in the refractive index with the increase in the

doping percentage with (ZnS), This is consistent with what was stated by researchers M. Golam Mortuza Nion and Payel Maiti [6, 8]. The reason for this increase is the density of the donor levels formed by the impurity within the energy gap, which leads to an increase in the intensity of the reflected rays and also an increase in the absorption coefficient, thus increasing the refractive index and the extinction coefficient [37, 38].

$$k_o = \frac{\alpha\lambda}{4\pi} \tag{3}$$

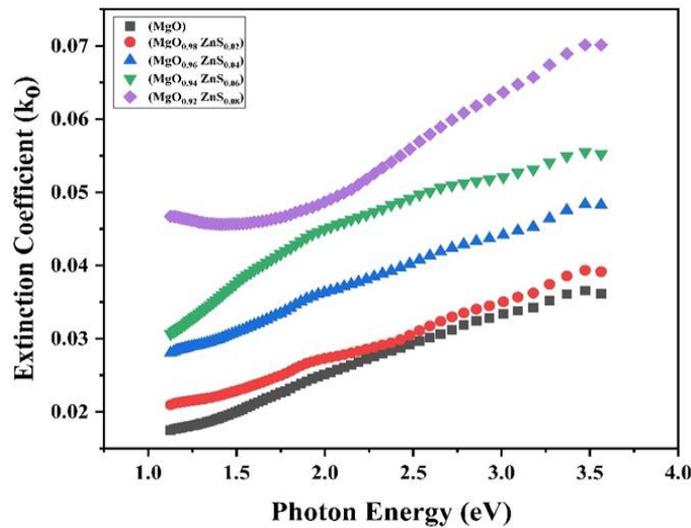$$n_o = \left[\left(\frac{1+R}{1-R}\right)^2 - (K_o^2 + 1)\right]^{1/2} + \frac{1+R}{1-R} \tag{4}$$

Fig. 7. Extinction Coefficient of MgO$_{1-x}$ZnS$_x$ thin films.
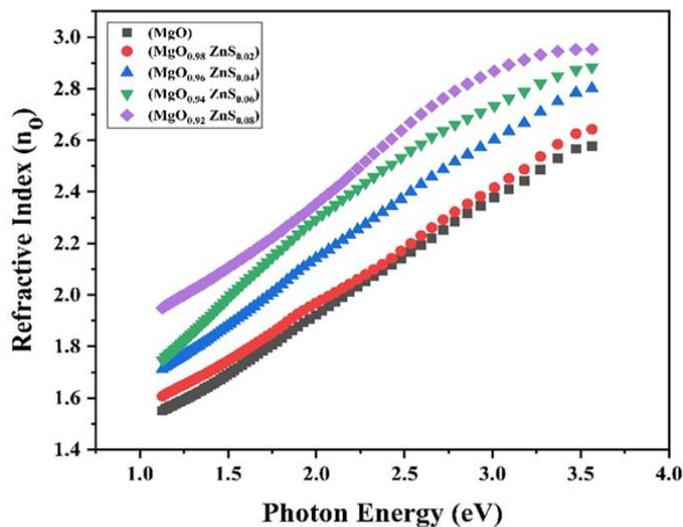

Fig. 8. Refractive Index of (MgO$_{1-x}$ZnS$_x$) thin films.

Fig. 9 shows the real dielectric constant and the imaginary dielectric constant, where the value of each increases with the increase in the percentage of doping with (ZnS). We note that the value of the imaginary dielectric constant is small compared to the value of the real dielectric constant for all the prepared films. This low value indicates that the energy dissipation for all the

prepared films is low. While the increasing value of the real dielectric constant represents the increase in the electric flux density of the prepared thin films [8, 17], Table 2. Shows the value of the optical energy gap and the highest values for the absorption coefficient, extinction coefficient, and refractive index for all prepared films.
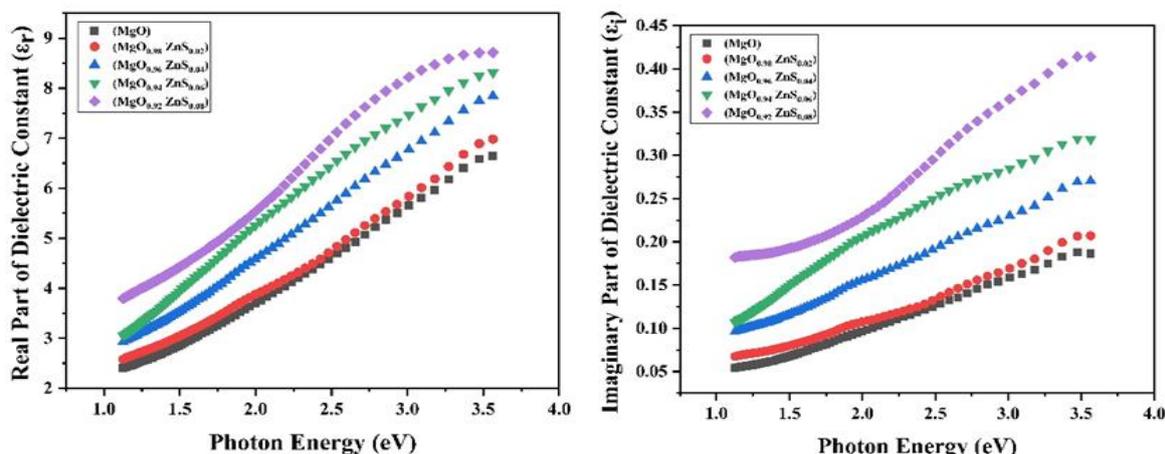

Fig. 9. Real Part of Dielectric Constant and Imaginary Part of Dielectric Constant of (MgO1-xZnSx) thin films.

Table 2. Optical properties for $(MgO_{1-x}ZnS_x)$ thin films at (350 °C).

Sample	Energy Gap (eV)	(α ×104 cm-1) Maximum	(ko) Maximum	)no(Maximum
MgO	2.771	1.304	0.036	2.577
$MgO_{0.98}ZnS_{0.02}$	2.714	1.413	0.039	2.642
$MgO_{0.96}ZnS_{0.04}$	2.638	1.742	0.048	2.801
$MgO_{0.94}ZnS_{0.06}$	2.602	1.993	0.055	2.883
$MgO_{0.92}ZnS_{0.08}$	2.549	2.531	0.070	2.952

4. Conclusions

(MgO) and (ZnS-doped) thin films were successfully fabricated on a glass substrate by the spray pyrolysis technique. It is observed that (ZnS-doping) concentration significantly affects the morphology and optical properties. The (AFM) results showed that the surface roughness values decreased with (ZnS) doping increase. Optical transmittance decreased with increasing (ZnS) doping. The energy gap of the (MgO) thin film was found to be around (2.771eV) and as low as (2.549eV) for the film impregnated with (8%) of (ZnS). The results obtained show a significant improvement in the morphology and optical properties of the (MgO) thin films, making them a helpful material in fabricating solar cells.

References

[1] G. Carta et al., Chemical vapor deposition, vol. 13, no. 4, pp. 185-189, 2007; https://doi.org/10.1002/cvde.200606574

[2] A. Moses Ezhil Raj, L. Nehru, M. Jayachandran, and C. Sanjeeviraja, Crystal Research and Technology: Journal of Experimental and Industrial Crystallography, vol. 42, no. 9, pp. 867-875, 2007; https://doi.org/10.1002/crat.200710918

[3] S. Visweswaran, R. Venkatachalapathy, M. Haris, and R. Murugesan, Journal of Materials

Science: Materials in Electronics, vol. 31, no. 17, pp. 14838-14850, 2020;
https://doi.org/10.1007/s10854-020-04046-7

[4] H. K. Yu, Thin Solid Films, vol. 653, pp. 57-61, 2018;
https://doi.org/10.1016/j.tsf.2018.03.014

[5] S. Benedetti, N. Nilius, and S. Valeri, The Journal of Physical Chemistry C, vol. 119, no. 45, pp. 25469-25475, 2015; https://doi.org/10.1021/acs.jpcc.5b09033

[6] P. Maiti et al., Materials Research Express, vol. 4, no. 8, p. 086405, 2017;
https://doi.org/10.1088/2053-1591/aa8279

[7] M. R. Islam, M. Rahman, S. Farhad, and J. Podder, Surfaces and Interfaces, vol. 16, pp. 120-126, 2019; https://doi.org/10.1016/j.surfin.2019.05.007

[8] M. G. M. Nion et al., Results in Materials, vol. 12, p. 100235, 2021;
https://doi.org/10.1016/j.rinma.2021.100235

[9] A. Goktas, A. Tumbul, Z. Aba, A. Kilic, and F. Aslan, Optical Materials, vol. 107, p. 110073, 2020; https://doi.org/10.1016/j.optmat.2020.110073

[10] M. Ashokkumar and A. Boopathyraja, Superlattices and Microstructures, vol. 113, pp. 236-243, 2018; https://doi.org/10.1016/j.spmi.2017.11.005

[11] I.-C. Ho, Y. Xu, and J. D. Mackenzie, Journal of Sol-Gel Science and Technology, vol. 9, no. 3, pp. 295-301, 1997; https://doi.org/10.1007/BF02437193

[12] T. K. Talukdar, S. Liu, Z. Zhang, F. Harwath, G. S. Girolami, and J. R. Abelson, Journal of Vacuum Science & Technology A: Vacuum, Surfaces, and Films, vol. 36, no. 5, p. 051504, 2018; https://doi.org/10.1116/1.5040855

[13] M. Saeed, M. Al-Timimi, and O. Hussein, Digest Journal of Nanomaterials and Biostructures, vol. 16, no. 2, pp. 563-569, 2021.

[14] T. Güngör, B. USLU, E. Güngör, and A. BÖBREK, Arduino Based Thin Film Spin Coating System Design and MgO Thin Film Preparation, 2020.

[15] M. Tlili, N. Jebbari, W. Naffouti, and N. T. Kamoun, The European Physical Journal Plus, vol. 135, no. 8, pp. 1-12, 2020; https://doi.org/10.1140/epjp/s13360-020-00706-z

[16] M. H. Kabir, A. Bhattacharjee, M. M. Islam, M. Rahman, M. Rahman, and M. Khan, Journal of Materials Science: Materials in Electronics, vol. 32, no. 3, pp. 3834-3842, 2021;
https://doi.org/10.1007/s10854-020-05127-3

[17] M. H. Kabir, M. Rahman, and M. Khan, Chinese Journal of Physics, vol. 56, no. 5, pp. 2275-2284, 2018; https://doi.org/10.1016/j.cjph.2018.07.004

[18] C.-Y. Tsay, H.-C. Cheng, Y.-T. Tung, W.-H. Tuan, and C.-K. Lin, Thin Solid Films, vol. 517, no. 3, pp. 1032-1036, 2008; https://doi.org/10.1016/j.tsf.2008.06.030

[19] T. Saidani, M. Zaabat, M. Aida, and B. Boudine, Superlattices and Microstructures, vol. 88, pp. 315-322, 2015; https://doi.org/10.1016/j.spmi.2015.09.029

[20] M. Ajili, M. Castagné, and N. K. Turki, Superlattices and Microstructures, vol. 53, pp. 213-222, 2013; https://doi.org/10.1016/j.spmi.2012.10.012

[21] M. D. Sakhil et al., NeuroQuantology, vol. 18, no. 5, p. 56, 2020;
https://doi.org/10.14704/nq.2020.18.5.NQ20168

[22] H. Güney and D. İskenderoğlu, Canadian Journal of Physics, vol. 96, no. 7, pp. 804-809, 2018; https://doi.org/10.1139/cjp-2017-0767

[23] F. T. Ibrahim, Iraqi Journal of Applied Physics, vol. 13, no. 3, 2017.

[24] A. T. Abood, O. A. A. Hussein, M. H. Al-Timimi, M. Z. Abdullah, H. M. S. Al Aani, and W. H. Albanda, in AIP Conference Proceedings, 2020, vol. 2213, no. 1: AIP Publishing LLC, p. 020036; https://doi.org/10.1063/5.0000454

[25] X. Liu, S. Chen, M. Li, and X. Wang, Thin Solid Films, vol. 515, no. 17, pp. 6744-6748, 2007; https://doi.org/10.1016/j.tsf.2007.02.004

[26] I. M. El Radaf, T. A. Hameed, and I. Yahia, Materials Research Express, vol. 5, no. 6, p. 066416, 2018; https://doi.org/10.1088/2053-1591/aaca7b

[27] M. Abdullal, R. Jaseen, and A. H. Resan, J. Pure Sciences, vol. 7, no. 3, pp. 205-213, 2011.

[28] I. R. Agool, K. J. Kadhim, and A. Hashim, International Journal of Plastics Technology, vol. 21, no. 2, pp. 397-403, 2017; https://doi.org/10.1007/s12588-017-9192-5

[29] A. Goswami, Thin film fundamentals. New age international, 1996.

[30] A. Louardi et al., Materials Focus, vol. 7, no. 4, pp. 459-463, 2018; https://doi.org/10.1166/mat.2018.1531

[31] S. Aksay, Physica B: Condensed Matter, vol. 570, pp. 280-284, 2019; https://doi.org/10.1016/j.physb.2019.06.020

[32] A. Taşer, M. E. Güldüren, and H. Güney, Ceramics International, vol. 47, no. 11, pp. 15792-15800, 2021; https://doi.org/10.1016/j.ceramint.2021.02.151

[33] A. Taşer, M. E. Güldüren, and H. Güney, Materials Chemistry and Physics, vol. 272, p. 124993, 2021; https://doi.org/10.1016/j.matchemphys.2021.124993

[34] R. Premarani, J. Jebaraj Devadasan, S. Saravanakumar, R. Chandramohan, and T. Mahalingam, Journal of Materials Science: Materials in Electronics, vol. 26, no. 4, pp. 2059-2065, 2015; https://doi.org/10.1007/s10854-014-2647-y

[35] M. H. Abdul-Allah, S. A. Salman, and W. H. Abbas, Journal of Thi-Qar Science, vol. 5, no. 1, 2014.

[36] S. O. Kasap, Principles of electronic materials and devices. McGraw-Hill New York, 2006.

[37] O. N. Ogada, Effect of concentration of reactants and deposition temperature on the optical properties of iron-doped cadmium stannate thin films deposited on glass substrates by spray pyrolysis, Maseno University, 2019.

[38] S. Chiad, N. Habubi, W. Abass, and M. Abdul-Allah, Journal of Optoelectronics and Advanced Materials, vol. 18, no. 9-10, pp. 822-826, 2016.